Optimizational 1.06 μm spectroscopic properties of $Na_5Lu_9F_{32}$ single crystals doped with Nd^{3+} ions

QIGUO SHENG[a], HAIPING XIA[a,*], QINGYANG TANG[a], SHINAN HE[a], BAOJIU CHEN[b]
[a]*Key laboratory of Photo-electronic Materials, Ningbo University, Ningbo, Zhejiang, 315211, China*
[b]*Department of Physics, Dalian Maritime University, Dalian, Liaoning Province, 116026, China*

The high quality $Na_5Lu_9F_{32}$ single crystals with different Nd^{3+} concentrations ranging from 0.5 to 4 mol% were grown successfully by an improved Bridgman method. The Judd-Ofelt intensity parameters Ω_t (t=2, 4, 6) were calculated based on the measured absorption spectra. The stimulated emission cross section (σ_{em}) from $^4F_{3/2}$ to $^4I_{11/2}$ transition (1.06 μm) for 1.0 mol% Nd^{3+} doped $Na_5Lu_9F_{32}$ single crystal is calculated to be 4.58×10^{-20} cm^2. The fluorescence spectra and decay curves at 1.06 μm were measured under the excitation of 808 nm LD to study the luminescent properties of the crystals. The 1.06 μm emission intensity gradually increases to the maximum value when the Nd^{3+} concentration increases to around 1.0 mol%. Nevertheless, it decreases fleetly with the Nd^{3+} concentration further increases from 2.0 mol% to 4.0mol%. The 1.06 μm fluorescence lifetime of Nd^{3+}: $^4F_{3/2}\rightarrow{}^4I_{11/2}$ level decreases with the increase of Nd^{3+} doping concentration. The concentration quenching effect of Nd^{3+} ions are mainly in charge of the variety of the 1.06 μm emission.

(Received June 29, 2017; accepted April 5, 2018)

Keywords: Nd^{3+} ion, $Na_5Lu_9F_{32}$ single crysta, Optical spectra, 1.06 μm

1. Introduction

Over the past decades, the synthesis and development of single crystals doped with rare ions are inducing intense interest because of their ordered rigid crystal lattice and high chemical-physical stability. As one kind of important rare earth ions, Nd^{3+} ion possesses a very intense absorption peak at around 800 nm, which is very corresponding to 808 nm LD laser wavelength commercially, so it can be effectively used as excitation source for semiconductor laser [1-3]. At the same time, in view of the long fluorescence lifetime and large stimulated emission cross section, the Nd^{3+} ion doped materials have been widely applied in laser technology, especially in the field of high power laser [4]. It is well known that the YAG crystals doped with Nd^{3+} ions are regarded as the most widely used laser materials [5-6].

In recent years, a lot of researches and developments of other crystals doped Nd^{3+} ion have been done [7-8]. It is worthwhile to note that Nd^{3+} doped $LiYF_4$ single crystals were successfully prepared by using an improved Bridgman method, and their excellent optical spectra were also observed [9]. Since fluoride hosts surpass oxide ones in minimum matrix phonon energy and transparency within the infrared wavelength range, it thus becomes possible to extend study beyond the limitations of oxide matrices [10-11].

As a fluoride compound, the $Na_5Lu_9F_{32}$ single crystals have been demonstrated to have good thermal stability and physical-chemical performance [12]. It plays an important role for the doped trivalent rare-earth ions in taking the place of the Lu^{3+} ions. On the other hand, its high optical transparency in the range of infrared and the lower phonon energy (400 cm^{-1}) [13] also makes $Na_5Lu_9F_{32}$ single crystal very suitable as potential laser material for the infrared laser devices. Although, some rare earth ions were incorporated in $Na_5Lu_9F_{32}$ single crystals and optical performances such as up-conversion were investigated [14], there are almost no reports on Nd^{3+} doped $Na_5Lu_9F_{32}$ single crystal for 1.06 μm laser.

In this work, $Na_5Lu_9F_{32}$ single crystals doped Nd^{3+} with various concentrations (0.5, 1, 2, 4 mol%) were grown successfully by an improved Bridgman method. The absorption spectra were measured and the J-O optical parameters were calculated. The emission spectrum of 1.06 μm and decay curve of Nd^{3+} singly doped $Na_5Lu_9F_{32}$ crystals were investigated. It is expected that this study provides a good theoretical basis for the further development and implementation of infrared devices.

2. Experimental

Bridgman method was used for growth of the Nd^{3+} doped $Na_5Lu_9F_{32}$ single crystals. The starting materials were commercially available powders of high purity NaF (99.99%), LuF_3 (99.99%) and NdF_3 (99.99%) purchased from the market. The molar ratio of $NaF:LuF_3:NdF_3$ is

50:50-χ:χ(χ=0.5, 1, 2, 4). The mixture was put into apparatus in anhydrous HF atmosphere for fluoridation processing for about 6-8h at 820 ℃ to fully remove moisture and impurities in the raw materials. The seed directed along c-axis was put in the bottom of seed well. The temperature gradient across the solid-liquid interface was 70-90 ℃/cm. The crystal growth process was carried out by descending the crucible at a rate of 0.08 mm/h, which would last about 8-10 days. The detailed description has been described elsewhere [15].

The insert of Fig. 1 shows the light pink boule of grown crystal in length of 30 mm and diameter of 10 mm and a polished piece. The X-ray diffraction (XRD) was recorded by using a XD-98X diffractometer (XD-3, Beijing). The real Nd^{3+} concentrations in single crystal were measured by an inductively coupled plasma atomic emission spectroscopy (ICP-AES PerkinElmerInc, Optima 3000). Table 1 lists the measured Nd^{3+} concentrations and the molar fractions of Nd^{3+} in raw material. A Cary 5000 UV/VIS/NIR spectrophotometer was used for measuring the absorption spectra. The emission spectra were recorded under the 808 nm LD excitation by a Triax 320 type spectrometer. The fluorescence lifetimes at 1.06 μm were recorded with FLSP920 fluorescence spectrophotometer. All these measurements were carried out at room temperature.

Table 1. Measured Nd^{3+} concentrations in single crystals and molar fractions of Nd^{3+} in starting materials

Samples	i	ii	iii	iv
Nd^{3+}/mol%	0.5mol%	1.0mol%	2.0mol%	4.0mol%
10^{20}N/cm^3	0.63	1.25	2.56	4.98

3. Results and discussions

The XRD pattern of the product synthesized by an improved Bridgman method of 2.0 mol% Nd^{3+} doped $Na_5Lu_9F_{32}$ single crystal is shown in Fig. 1. The other Nd^{3+} doped samples also exhibit similar XRD characteristics without no obvious difference. Compared with peak positions of JCPDS cards (27-0725) of $Na_5Lu_9F_{32}$ crystal shown in Fig. 1 (c), the diffraction peaks and relative intensities of the as-prepared samples are roughly consistent with the standard line patterns. The narrow diffraction peaks express the formation of pure cubic phase of the obtained crystal. The calculated cell parameters for 2.0 mol% Nd^{3+} doped $Na_5Lu_9F_{32}$ crystal as shown in Fig. 1(b) are a=b=c=0.5465 nm. One can confirm the $Na_5Lu_9F_{32}$ single crystals were highly transparent since the transmittance was measured to be ~90% in the visible region and no grain boundary was observed.

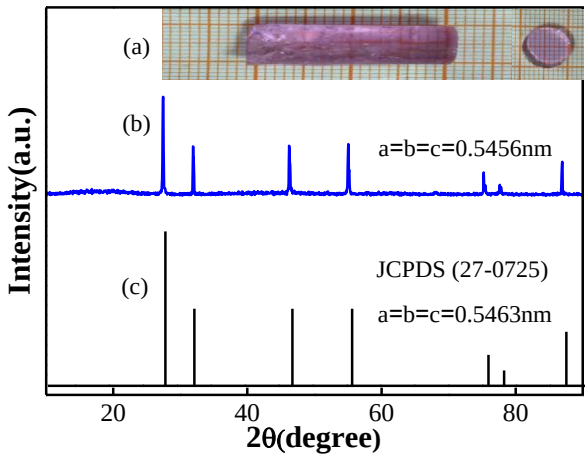

Fig. 1. (a) The insert is the photograph of Nd^{3+} doped $Na_5Lu_9F_{32}$ single crystal and a polished piece. (b) XRD pattern of the 2mol% Nd^{3+} doped $Na_5Lu_9F_{32}$ crystal. (c) $Na_5Lu_9F_{32}$ standard line pattern

Fig. 2 illustrates the absorption spectra of various Nd^{3+} doped $Na_5Lu_9F_{32}$ crystals in the wavelength ranging from 400 nm to 1000 nm. It can be observed from Fig. 2 that the absorption intensities increase gradually with the continuous increase of the Nd^{3+} doping concentration from 0.5 mol% to 4.0 mol%, while the positions of the peaks remain unchanged. Absorption bands are labeled for Nd^{3+} ions corresponding to transitions from the ground state to upper states. It can be seen from Fig. 2 that there are six obvious absorption bands of Nd^{3+} located at 521, 577, 676, 733, 795 and 865 nm, which is respectively corresponded to the transitions from the ground state $^4I_{9/2}$ to the excited states $^4G_{7/2}$, $^4G_{5/2}$ ($^2G_{7/2}$), $^4F_{9/2}$, $^4F_{7/2}$ ($^4S_{3/2}$), $^4F_{5/2}$ ($^2H_{9/2}$) and $^4F_{3/2}$ of Nd^{3+} ions.

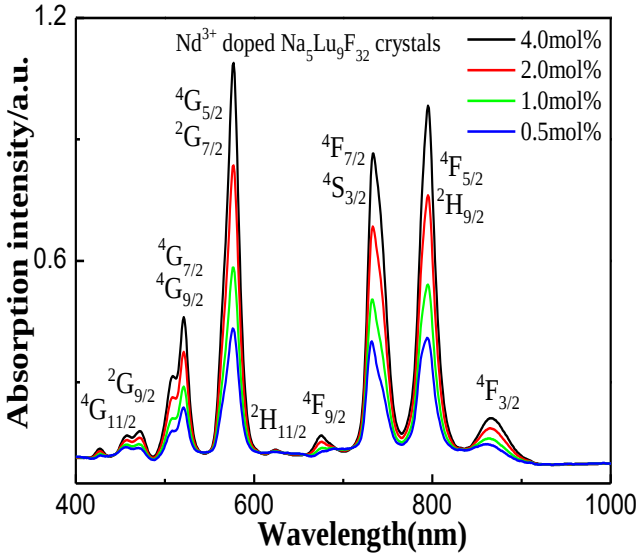

Fig. 2. Absorption spectra of Nd^{3+} doped $Na_5Lu_9F_{32}$ single crystals with various concentrations

According to Judd-Ofelt theory [16-17], the calculated oscillator strengths are obtained by the following expression:

$$f_{cal} = f_{ed} + f_{md} \tag{1}$$

$$f_{ed} = \frac{8mc\pi^2}{3h\lambda(2J+1)} \times \frac{(n^2+2)^2}{9n} \times \sum_{t=2,4,6} \Omega_t \left| \left\langle 4f^N[S,L]J \left\| U^{(t)} \right\| 4f^N[S',L']J' \right\rangle \right|^2 \tag{2}$$

$$f_{md} = \frac{h}{6mc\lambda(2J+1)} \times \frac{(n^2+2)^2}{9n} \times \left| \left\langle 4f^N[S,L]J \left\| L+2S \right\| 4f^N[S',L']J' \right\rangle \right|^2 \tag{3}$$

where n is the refractive index of sample, λ is the wavelength of the absorption peak, h is the Planck constant, J and J' are the total angular momentum quantum number of the initial and final states and $\left| \left\langle 4f^N[S,L]J \left\| U^{(t)} \right\| 4f^N[S',L']J' \right\rangle \right|$ is the reduced matrix elements.

The root-mean-square (RMS) deviation of the experimental and calculated oscillator strengths is defined by

$$\delta = \sqrt{\frac{\sum_{i=0}^{M} (f_{cal} - f_{exp})^2}{M-3}} \tag{4}$$

where M is the number of absorption bands involved in the calculation of the measured line strengths.

Judd-Ofelt parameters Ωt (t=2, 4, 6) can be calculated by Judd-Ofelt theory. The results of *RMS* deviation for δ and the experimental and calculated oscillator strengths of Nd^{3+} ion from the ground state ($^4I_{9/2}$) to different excited states in the $Na_5Lu_9F_{32}$ crystal are listed in Table 2.

Table 2. The experimental and calculated oscillator strengths of Nd^{3+}: $Na_5Lu_9F_{32}$

J	$\rightarrow J'$	λ (nm)	A_{ed}/s^{-1}	A_{md}/s^{-1}	∑A	β	τ_{rad} (ms)
$^4I_{11/2}$	$\rightarrow ^4I_{9/2}$	5313.5	11.50	1.67	13.17	1.00	75.93
$^4I_{13/2}$	$\rightarrow ^4I_{11/2}$	5053.1	12.34	2.21	43.31	0.33	23.09
	$\rightarrow ^4I_{9/2}$	2585.3	28.76			0.67	
$^4I_{15/2}$	$\rightarrow ^4I_{13/2}$	4852	35.68	1.64	133.05	0.28	7.52
	$\rightarrow ^4I_{11/2}$	2480.2	71.60			0.54	
	$\rightarrow ^4I_{9/2}$	1689.2	24.13			0.18	
$^4F_{3/2}$	$\rightarrow ^4I_{15/2}$	1828.5	18.34		3676.3	0.005	0.28
	$\rightarrow ^4I_{13/2}$	1324.2	341.25			0.09	
	$\rightarrow ^4I_{11/2}$	1052.2	1759.5			0.48	
	$\rightarrow ^4I_{9/2}$	868.4	1557.2			0.43	

The obtained Judd-Ofelt parameters compared with Nd^{3+} doped other crystals are also presented in Table 3.

The value of Ωt is closely related to the matrix structure, the symmetry and the order of the vicinity of rare earth ions in the crystals. According to Judd-Ofelt theory, the symmetry of crystal structure is much higher and the electrovalent bond is stronger when the value of $\Omega 2$ is much lower. Meanwhile, $\Omega 2$ is sensitive to the environmental configuration symmetry of rare earth ions and it will decrease with the varying of host material from oxide to fluoride. As is shown in Table 3, the value of $\Omega 2$ in $Na_5Lu_9F_{32}$ crystal is lower than Nd^{3+} doped other materials. This comparison confirmed that the symmetry of $Na_5Lu_9F_{32}$ crystal structure is much stricter.

Table 3. Comparison of the Judd-Ofelt parameters for Nd^{3+} doped materials

Transition: $^4I_{9/2} \rightarrow$	Wavelength(nm)	Oscillator strengths(10^{-6}) f_{exp}	f_{cal}
$^4F_{3/2}$	865	0.361	0.33
$^4F_{5/2}$, $^2H_{9/2}$	795	1.461	1.723
$^4F_{7/2}$, $^4S_{3/2}$	733	1.444	1.012
$^4F_{9/2}$	676	0.274	0.205
$^4G_{5/2}$, $^2G_{7/2}$	577	5.7	5.76
$^4G_{7/2}$	521	2.234	0.836
$\delta_{rms}(10^{-6})$		0.85	

Once the intensity parameters are obtained, the electric dipole transition rate A_{ed} from J manifold to lower energy J' manifold can be expressed by:

$$A_{ed} = \frac{64\pi^4 e^2}{3h\lambda^3(2J+1)} \times \frac{n(n^2+2)^2}{9} \times \sum_{t=2,4,6} \Omega_t \left| \left\langle 4f^N[S,L]J \left\| U^{(t)} \right\| 4f^N[S',L']J' \right\rangle \right|^2 \quad (5)$$

The magnetic dipole transition rate A_{md} by using following equation:

$$A_{md} = \frac{64\pi^4 e^2}{3h\lambda^3(2J+1)} \times \frac{h^2 n^3}{16m^2c^2\pi^2} \times \left| \left\langle 4f^N[S,L]J \left\| L+2S \right\| 4f^N[S',L']J' \right\rangle \right|^2 \quad (6)$$

The transition rate A can be deduced by $A(J, J') = A_{ed} + A_{md}$. The fluorescence branching ratio β and the radiative lifetime τ_{rad} can be respectively calculated by:

$$\beta = \frac{A[(S,L)J,(S',L')J']}{\sum_{S'L'J'} A[(S,L)J,(S',L')J']} \quad (7)$$

$$\tau_{rad} = \frac{1}{\sum_{S'L'J'} A[(S,L)J,(S',L')J']} \quad (8)$$

All results calculated by above formulas are listed in the Table 4.

Table 4. The value of the calculated A, β, τ_{rad} of Nd^{3+}: $Na_5Lu_9F_{32}$ crystal

Crystals	$\Omega_2/10^{-20}cm^2$	$\Omega_4/10^{-20}cm^2$	$\Omega_6/10^{-20}cm^2$	Reference
Fluoro-phosphate glass	8.04	1.47	7.67	[18]
Fluorogallate	6.42	4.16	3.71	[19]
Phosphate	5.27	3.69	4.31	[20]
Tellurite	4.71	4.06	3.89	[21]
$Na_5Lu_9F_{32}$	4.58	0.67	4.31	This work

Fig. 3 presents the emission spectra with the variation of Nd^{3+} doped concentrations from 850 to 1400 nm wavelength via excited by 808 nm LD at room temperature. In these emission spectra, there are three clear fluorescence emission peaks at around 868 m, 1052 nm (relatively weak) and 1324nm, which are related to Nd^{3+} transitions $^4F_{3/2} \rightarrow {}^4I_{9/2}$, $^4F_{3/2} \rightarrow {}^4I_{11/2}$ and $^4F_{3/2} \rightarrow {}^4I_{13/2}$, respectively. As common output wavelength of the laser, the 1052 nm fluorescence intensity is the highest among these transitions. It can be concluded from Fig. 3 that under the excitation of 808 nm LD, Nd^{3+} at the ground state transfers to the excited states of $^4F_{5/2}$ and $^2H_{9/2}$, soon after non-radiatively transferring to metastable state $^4F_{3/2}$. Above-mentioned three kinds of fluorescence were produced during the transition process from the $^4F_{3/2}$ to the lower levels, and then returns to the ground state. The energy level diagram depicting the excitation and emission transitions of Nd^{3+} doped $Na_5Lu_9F_{32}$ single crystal is shown in Fig. 4 [22].

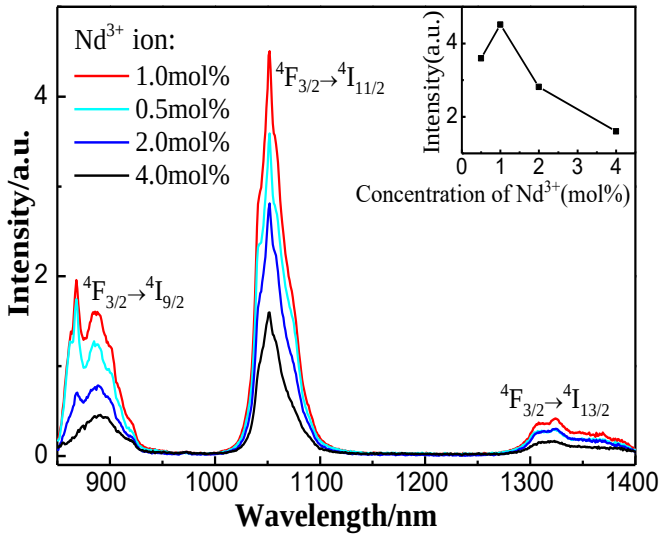

Fig. 3. Emission spectra of the Nd^{3+} doped $Na_5Lu_9F_{32}$ single crystals excited by 808 nm LD

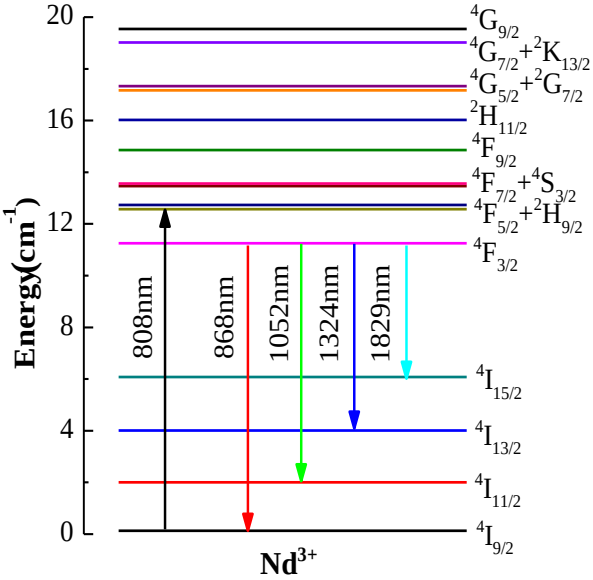

Fig. 4. The simplified energy level diagram of Nd^{3+}:$Na_5Lu_9F_{32}$ crystal

It is clear that the beginning fluorescence emission intensity at 1052 nm is gradually increasing with the doping concentration of Nd^{3+} increased from 0.5 mo% to 1.0 mol%, then begins to drop dramatically when the concentration continues to rise from 1.0mol% to 4.0 mol% due to the concentration quenching effect of Nd^{3+} ions. It indicates that the optimizational concentration of Nd^{3+} in $Na_5Lu_9F_{32}$ single crystal to obtain 1.06 μm emission is about ~1.0 mol%.

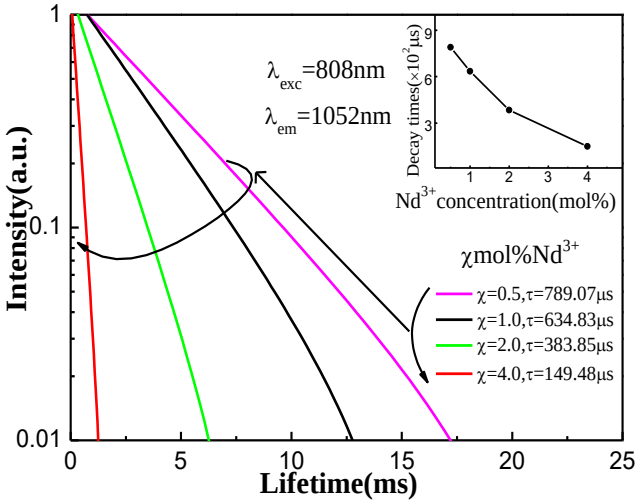

Fig. 5. Fluorescence decay curves at 1052 nm of Nd^{3+} ion in $Na_5Lu_9F_{32}$ single crystals. The inset is the decay times dependence on Nd^{3+} concentration

Fig. 5 presents the normalized fluorescence decay curves of the $^4F_{3/2}$ level for the $Na_5Lu_9F_{32}$ crystals with various Nd^{3+} concentrations excited by 808 nm LD. The curves can be well fitted by using a single exponential function:

$$I(t)/I(0) = \exp(-t/\tau_{fit}) \quad (9)$$

where *I(t)*, *I0* represent the luminescence intensities at the time *t* after the cutoff the excitation light and the initial emission intensity at t=0, and τ_{fit} is fitting lifetimes. The fluorescence lifetimes were obtained from the decay curves, they are 789.07μs, 634.83μs, 383.85μs, 149.48μs for 0.5 mol%, 1.0 mol%, 2.0mol%, 4.0 mol% Nd^{3+} doping samples. Obviously, the lifetime of Nd^{3+} in $Na_5Lu_9F_{32}$ is longer than that in YAG, and near to that in other fluoride compounds [23]. The inset of Fig. 5 is the 1052 nm emission decay times dependence on Nd^{3+} concentration. It can be noted that as the Nd^{3+} concentration increases the fluorescence lifetime at 1052 nm emission decreases.

The stimulated emission cross section is one of the vital parameters to assess the performance of a laser crystal and its value signifies the rate of energy extraction from the lasing material. The absorption cross section (σ_{abs}) of Nd^{3+} from $^4I_{9/2}\rightarrow{}^4F_{5/2}$ transition at 795 nm can be estimated from the absorption spectrum of Nd^{3+} doped $Na_5Lu_9F_{32}$ single crystal by using following equation.

$$\sigma_{abs(\lambda)} = \frac{2.303OD(\lambda)}{NL} \quad (10)$$

Where *N* is the number of Nd^{3+} ion per unit volume (cm^{-3}), *OD(λ)* is the optical density as a function of wavelength *λ*, and *L* is the thickness of the sample, *λ* is the wavelength.

The stimulated emission cross section (σ_{em}) of Nd^{3+} from $^4F_{3/2}\rightarrow{}^4I_{11/2}$ transition at 1.06 μm can be calculated from the fluorescence spectrum by McCumber theory [24] as:

$$\sigma_{em}(\lambda) = \sigma_{abs}(\lambda)\exp[\frac{\varepsilon - hc\lambda^{-1}}{kT}] \quad (11)$$

Where *T* is temperature (here is the room temperature), *k* is the Boltzmann constant (1.38×10-23J/K), *h* is the Planck

constant, λ is the transition wavelength, c is the light velocity, ε represents energy difference between the lowest Stark levels of $^4F_{3/2}$ and $^4I_{11/2}$ two multiplets at room temperature (for $^4F_{3/2}\rightarrow{}^4I_{11/2}$ transition of Nd^{3+}, $\varepsilon \approx 9503.9$ cm^{-1}).

The calculated σ_{abs} transiting from $^4I_{9/2}$ to $^4F_{5/2}$ and σ_{em} from $^4F_{3/2}$ to $^4I_{11/2}$ for 1.0mol% Nd^{3+} doped $Na_5Lu_9F_{32}$ single crystal are equal to 1.29×10-20 cm^2 and 4.58×10-20 cm^2, respectively. Compared with other Nd^{3+} doped matrices, this high value of emission cross section is larger than that in fluoro-phosphate (3.69×10-20 cm^2), phosphate glass (4.12×10-20 cm^2), tellurite glass (3.89×10-20 cm^2) [25]. Hence, this relatively high value indicates a possible application of the Nd^{3+}:$Na_5Lu_9F_{32}$ single crystal as an suitable working-laser material operating at 1.06 μm. Nevertheless, it should be noticed that the presented results are a subject to errors arising from the imperfection of the Judd-Ofelt theory and requiring further verification by laser experiments [26].

4. Conclusions

Our experiment demonstrated that Bridgman method is a favorable way to grow Nd^{3+} doped $Na_5Lu_9F_{32}$ single crystals. The maximum emission intensity at 1.06μm can be reached when the doping concentration of Nd^{3+} is ~1.0mol%. The measured maximum fluorescent lifetime at 1.06μm is 789.07μs. The stimulated emission cross section (σ_{em}) from $^4F_{3/2}$ to $^4I_{11/2}$ transition (1.06 μm) for 1.0 mol% Nd^{3+} doped $Na_5Lu_9F_{32}$ single crystal is calculated to be 4.58×10^{-20} cm^2. These excellent spectral parameters of Nd^{3+} doped $Na_5Lu_9F_{32}$ single crystals indicated that it may be a potential material for 1.06 μm laser.

Acknowledgments

This work was supported by the National Natural Science Foundation of China (Grant Nos. 51772159, 51472125), the Natural Science Foundation of Zhejiang Province (Grant No. LZ17E020001), and K. C. Wong Magna Fund in Ningbo University.

References

[1] I. Iparraguirre, J. Azkargorta, R. Balda, K. Venkata Krishnaiah, C. K. Jayasankar, M. Al-Saleh, J. Fernandez, Optics Express **19**, 19440 (2011).
[2] S. S. Li, P. Y. Wang, H. P. Xia, J. T. Peng, L. Tang, Y. P. Zhang, H. C. Jiang, Chinese Optics Letters **12**, 021601 (2014).
[3] Martin Frenz, Hans Pratisto, Flurin Konz, E. Duco Jansen, Ashley J. Welch, Heinz P. Weber, IEEE J. Quantum Electron **32**, 2025 (1996).
[4] Lili Hu, Dongbing He, Huiyu Chen, Xin Wang, Tao Meng, Lei Wen, Junjiang Hu, Yongchun Xu, Shunguang Li, Youkuo Chen, Wei Chen, Shubin Chen, Jingping Tang, Biao Wang, Optical Matreials **63**, 213 (2017).
[5] R. Boulesteix, A. Maitre, J. F. Baumard, Y. Rabinovitch, F. Reynaud, Optics Express **18**, 14992 (2010).
[6] C. L. Sung, H. P. Cheng, C. Y. Lee, C. Y. Cho, H. C. Liang, Y. F. Chen, Optics Letters **41**, 1781 (2016).
[7] Shoujun Ding, Qingli Zhang, Fang Peng, Wenpeng Liu, Jianqiao Luo, Renqin Dou, Guihua Sun, Xiaofei Wang, Dunlu Sun, Journal of Alloys and Compounds **25**, 159 (2017).
[8] J. Q. Hong, L. H. Zhang, P. X. Zhang, Y. Q. Wang, Y. Hang, Journal of Alloys and Compounds **646**, 706 (2015).
[9] Xiaobo Zhuang, Haiping Xia, Haoyang Hu, Jianxu Hu, Peiyuan Wang, Jiangtao Peng, Yuepin Zhang, Haochuan Jiang, Baojiu Chen, Materials Science and Engineering B **178**, 326 (2013).
[10] L. J. Li, B. Q. Yao, C. W. Song, Y. Z. Wang, Z. G Wang, Laser Phys. Lett. **6**, 102 (2009).
[11] Jun Izawa, Hayato Nakajima, HiroshiHara, Yoshinori Arimoto, Appl. Opt. **39**, 2418 (2000).
[12] R. Lv, P. Yang, Y. Dai, S. Gai, F. He, J. Lin, ACS Appl. Mat. Interfaces **6**, 15550 (2014).
[13] I. M. Shmyt'ko, G K. Strukova, Phys. Solid. State **51**, 1907 (2009).
[14] Cheng Wang, Haiping Xia, Zhigang Feng, Zhixiong Zhang, Dongsheng Jiang, Xuemei Gu, Yuepin Zhang, Baojiu Chen, Haochuan Jiang, Journal of Alloys and Compounds **686**, 816 (2016).
[15] Z. G Feng, H. P. Xia, C. Wang, Z. X. Zhang, D. S. Jiang, J. Zhang, S. N. He, Q. Y. Tang, Q. G sheng, X. M. Gu, Y. P. Zhang, B. J. Chen, H. C. Jiang, Chem. Phys. Lett. **652**, 68 (2016).
[16] B. R. Judd, Phys. Rev. **127**, 750 (1962).
[17] G S. Ofelt, J. Chem. Phys. **37**, 511 (1962).
[18] Y. C. Ratnakaram, S. Babu, L. Krishna Bharat, C. Nayak, Journal of Luminescence **175**, 57 (2016).
[19] Tianfeng Xue, Liyan Zhang, Junjiang Hu, Meisong Lia, Lili Hu, Opt. Mater. **47**, 24 (2015).
[20] G Takebe, Y. Nageno, K. Morinaga, J. Am. Chem. Soc. **78**, 2287 (1995).
[21] H. Kalaycioglu, H. Cankaya, G Ozen, L. Ovecoglu, A. Sennaroglu, Opt. Commun. **281**, 6056 (2008).
[22] Rasool Sk. Nayab, T. Sasikala, A. Mohan Babu, L. Rama Moorthy, C. K. Jayasankar, Spectrochimica Acta Part A: Molecular and Biomolecular Spectroscopy **180**, 193 (2017).
[23] Larry D. Merkle, Mark Dubinskii, Kenneth L. Schepler, S. M. Hegde, Optics Express **14**, 3893 (2006).
[24] B. Peng, T. Izumitani, Opt. Mater. **4**, 797 (1995).
[25] Y. C. Ratnakaram, S. Babu, L. Krishna Bharat, C. Nayak, Journal of Luminescence **175**, 57 (2016).
[26] Marcin Sobczyk, Damian Szymanski **183**, 226 (2017).

*Corresponding author: hpxcm@nbu.edu.cn